

Dipole-dipole interactions in potassium chloride doped with hydroxyl

R. C. Potter and A. C. Anderson

*Physics Department and Materials Research Laboratory,
University of Illinois at Urbana-Champaign, Urbana, Illinois 61801*

(Received 8 January 1981)

The dielectric constant $\epsilon = \epsilon' - i\epsilon''$ of KCl doped with OH^- or OD^- has been measured within the temperature range 0.1–250 K, the frequency range $10^2 - 10^5$ Hz, and the concentration range 0–4000 at. ppm. Discrete features appear in both ϵ' and ϵ'' which are related to a thermally activated, two-step reorientation of OH^- pairs. No evidence is found for a phase transition.

INTRODUCTION

The low-temperature behavior of the OH^- substitutional impurity in alkali halides has been studied extensively,^{1,2} partly because an associated electric dipole moment makes experimental observations relatively simple. In KCl crystals the dipoles are constrained to align along [100] directions,³ but can quantum-mechanically tunnel very rapidly between these six orientations. KCl:OH is therefore paraelectric at finite frequencies for temperatures above ≈ 5 K. At lower temperatures the energy of the average dipole-dipole interaction exceeds kT , the dipoles are “frozen” by the local fields,⁴ and the dielectric constant ϵ' is observed to pass through a maximum with decreasing temperature.⁵

The question has been raised as to whether the dipolar interaction can cause a phase transition. A mean-random-field calculation⁶ has indicated that a phase transition might occur for an OH^- concentration of ≥ 500 ppm. The signature of this transition would be a discontinuity in the temperature derivative of ϵ' somewhere near the maximum in ϵ' . Some evidence for a concentration-dependent discontinuity in $d\epsilon'/dT$ for KCl:OH did exist,^{7,8} and we therefore undertook an experimental study of this question. We have indeed observed discontinuities in $d\epsilon'/dT$ and have found these features to be related to interactions between the OH^- impurities. But they do not provide evidence for a phase transition. Rather, the features observed are caused by the “freezing” of explicit sets of dipole pairs.

EXPERIMENTAL DETAILS

The crystals⁹ were cleaved or cut to the dimensions of roughly $1 \times 1 \times 0.05$ cm³, with the small-

est dimension parallel to a [100] direction. Electrodes of silver paint or vapor-deposited indium were applied to within ≈ 0.05 cm of each edge. The crystals were mounted in a stress-free configuration between spring-loaded electrical contacts which also provided thermal contact.¹⁰ When not in the cryostat, the crystals were stored in a desiccator.

Both the capacitance C and the conductance G were measured for each sample using a three-terminal ratio-transformer capacitance bridge and a dual synchronous detector. Coaxially guarded leads ran from the bridge to the sample passing continuously through all vacuum feedthroughs. Both inner and outer conductors of each coax were thermally grounded within the cryostat to prevent heat leaks to the sample. Two sets of these electrical leads permitted the measurement of two samples during each cryogenic run. As a test of stability, the capacitance of a crystalline sapphire sample was measured¹⁰ over a voltage range of 0.06–6 V, a frequency range of $10^2 - 10^4$ Hz, and a temperature range of 0.02–10 K. The capacitance was found to be constant to within 2×10^{-4} . During measurements on KCl:OH, the voltage was kept sufficiently small so that the sample was not heated.

Temperatures were measured using a germanium resistance thermometer. This was calibrated against a set of superconducting fixed points¹¹ using a magnetic thermometer¹² for interpolation of the temperature scale.

The capacitance C and the conductance G were measured as a function of temperature T and angular frequency ω for a series of KCl crystals containing 80, 250, 500, 1500, or 4000 at. ppm OH^- , or 250 or 2000 ppm OD^- . The real and imaginary parts, ϵ' and ϵ'' , of the complex dielectric constant $\epsilon = \epsilon' - i\epsilon''$ were computed from the relations

$\epsilon' = C/C_0$ and $\epsilon'' = G/\omega C_0$. The constant C_0 is the capacitance with the entire KCl sample "removed." The determination of C_0 will be discussed below. As an example of our results, Fig. 1 shows the temperature dependence of ϵ' for a sample containing 1500 ppm OH^- . The temperature dependence of ϵ'' for this sample is shown in Fig. 2. For "pure" KCl with no intentional doping of OH^- , we found ϵ' to vary by less than 0.3% between 1 and 20 K.

We have used the temperature T_{max} at the center of the broad maximum in ϵ' to gauge the OH^- content of our samples.¹³ For the sample of Fig. 1 this temperature is 1.1 K. Figure 3 shows a plot of T_{max} versus OH^- concentration c obtained by several workers.^{5,7,14-16} The solid line represents a linear relationship between T_{max} and c , and is the empirical relationship we have used to obtain c from the T_{max} of our samples. This linear dependence between T_{max} and c is predicted theoretically,⁴ at least in the limit of low frequencies.

A second measure of OH^- concentration is obtained from the magnitude of the paraelectric response of each sample. As will be discussed further in the next section, the dielectric response of KCl:OH is closely paraelectric over a range of temperatures between roughly 5 and 100 K. That is, within this temperature range $C = C_m + \beta T^{-1}$, where C_m is the capacitance of the sample with no contribution from OH^- and where $\beta \propto p^2 c$, with p being the electric dipole moment of an OH^- ion in KCl. The slope of a plot of C versus T^{-1} provides values for β , and these values are indeed proportional to T_{max} . In brief, the OH^- concentrations quoted in this paper are linearly related to the actual concentrations, and the constant of proportionality

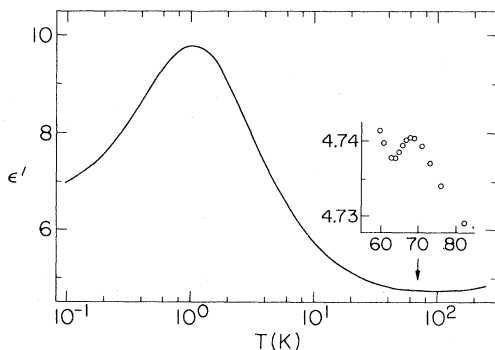


FIG. 1. Real part ϵ' of the dielectric constant of a KCl crystal containing 1500 ppm OH^- , measured at a frequency of 4×10^3 Hz. The inset shows a portion of the curve near 70 K with the vertical scale expanded by a factor of 160.

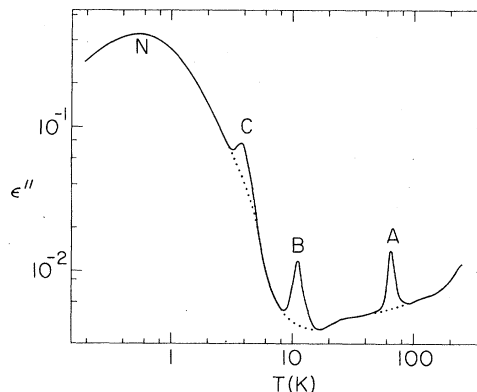


FIG. 2. Imaginary part ϵ'' of the dielectric constant of a KCl crystal doped with 1500 ppm OH^- , measured at a frequency of 4×10^3 Hz. The peaks A, B, C, and N are discussed in the text.

is the average of those obtained by previous workers who attempted to measure OH^- concentrations experimentally.

The intercepts from plots of C versus T^{-1} at $T^{-1} = 0$ provide values of C_m . Using a value¹⁷ of

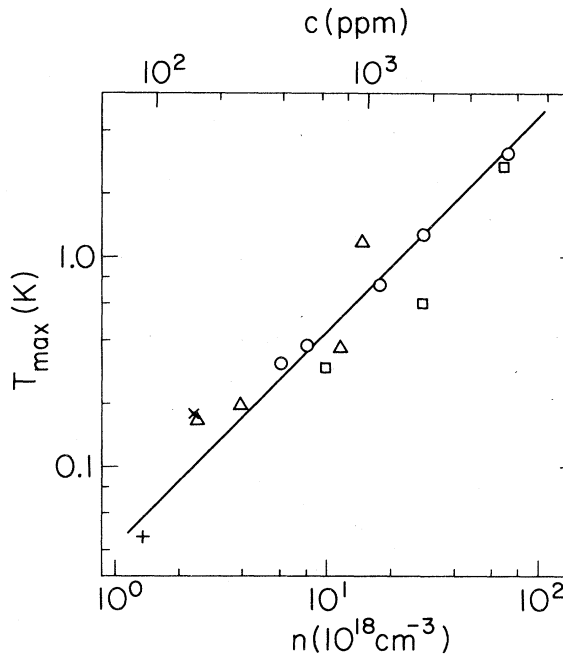


FIG. 3. Temperature T_{max} at which a broad maximum occurs in ϵ' , versus concentration c or density n of OH^- ions. Δ , Ref. 16; \circ , Ref. 14; $+$, Ref. 15; \times , Ref. 7; \square , Ref. 5. These results were not obtained at the same frequency. However, normalizing to the same frequency does not change the scatter relative to the line which is drawn with a slope of 1. The concentration and density are related by the expression $c = n/n_{\text{Cl}}$ where n_{Cl} is the number of Cl^- sites, $n_{\text{Cl}} = 1.6 \times 10^{22} \text{ cm}^{-3}$.

$\epsilon'_m = 4.5$ for pure KCl, $C_0 = C_m/4.5$. This procedure for obtaining C_0 , the constant used in the computation of ϵ' and ϵ'' , agrees within 5% with values calculated from the measured dimensions of the plated samples.

RESULTS AND DISCUSSION

The dielectric constant ϵ' of Fig. 1 does behave paraelectrically over much of the temperature range. That is, for the restricted temperature range the dielectric constant may be expressed in the simplified form

$$\epsilon' = \epsilon'_m + bT^{-1}, \quad (1)$$

where ϵ'_m is again the dielectric constant of pure KCl and b is proportional to the OH^- concentration. The T^{-1} behavior breaks down at temperatures below ≈ 5 K because of interactions between the electric dipole moments associated with the OH^- sites.^{4,5} At temperatures above ≈ 100 K, ϵ' begins to increase with increasing temperature. This increase is a property of ϵ'_m of Eq. (1) and is caused by anharmonic effects.¹⁸

Closer scrutiny of the data of Fig. 1 reveals small deviations from the temperature dependence of Eq. (1). One example is shown by the inset of Fig. 1. The magnitude of the temperature variation, shown by the inset, decreases with decreasing OH^- concentration. This indicates that the phenomenon seen in the inset is caused by the OH^- impurity and suggests that motion of some small subset of the OH^- population is being "frozen" as the temperature is reduced below ≈ 66 K. The majority of OH^- ions continue to behave paraelectrically and follow the applied alternating electric field. Therefore a more sensitive probe of the phenomenon is provided by ϵ'' , which detects only the subset of OH^- ions which are being frozen within the time scale ω^{-1} of the measurement. Indeed, Fig. 2 does show a peak in ϵ'' at 66 K. Similar features are found in ϵ'' (and in ϵ') near 25, 11, and 3.9 K. The broad peak labeled N in Fig. 2 is associated with the broad maximum in ϵ' near 1 K in Fig. 1. As will be shown below, the narrow peaks labeled A , B , and C in Fig. 2 vary in magnitude with OH^- concentration. The small peak near 25 K does not scale with OH^- concentration, it is probably caused by some trace impurity and will not be considered further. The peaks labeled B and C in Fig. 2 also appear in the data of Ref. 14.

The amplitudes of the three peaks labeled $A - C$

have been plotted in Fig. 4 as a function of OH^- or OD^- concentration. The amplitudes $\delta\epsilon''$ have been obtained by subtracting the background, the dotted line in Fig. 2, from the measured ϵ'' . From Fig. 4 it may be observed that $\delta\epsilon'' \propto c^2$. This fact indicates that the features under consideration are to be associated with dipole pairs. The only significant deviation is for the 4000 ppm OH^- sample, a concentration close to the limit for OH^- in KCl. At larger concentrations the shape of the maximum in ϵ' changes¹⁴ indicating that a linear relationship between T_{max} and c may not be valid at $c \gtrsim 4000$ ppm.

The temperatures T_p at which the peaks $A - C$ occur are *not* a function of concentration, but they are a function of frequency. Figure 5 shows the temperature measured at the center of peak B of the 1500 ppm OH^- sample as a function of the measuring frequency. The data obey the Arrhenius relation $\omega = \omega_{0B} e^{-\Delta_B/T}$ suggesting that the dipole pairs attempt to follow the direction of the applied

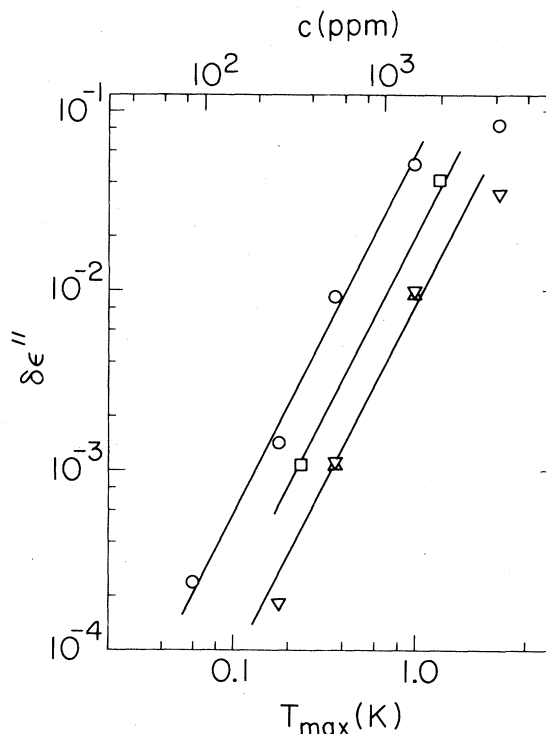


FIG. 4. The magnitude $\delta\epsilon''$ of the peak in Fig. 2, versus concentration of OH^- or OD^- . For OH^- : Δ , peak A ; ∇ , peak B ; \circ , peak C . For OD^- , \square is the equivalent of peak C . All data are for a measuring frequency of 10^4 Hz. The solid lines are drawn with a slope of 2.

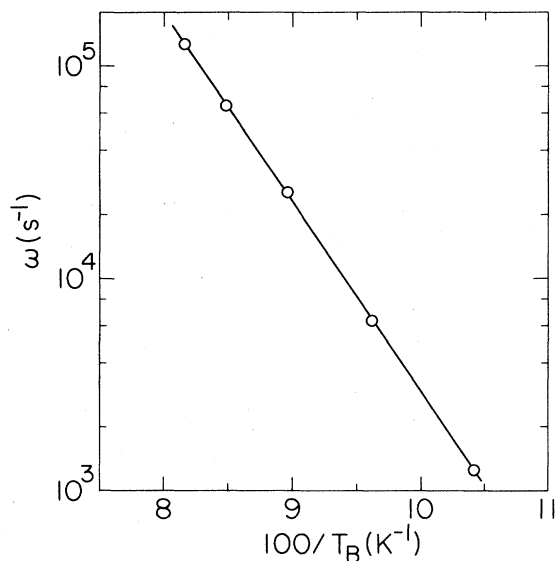


FIG. 5. Angular frequency ω at which peak B of Fig. 2 appears at temperature T_B for the 1500-ppm OH^- sample.

time-dependent electric field via a thermally activated reorientation process. That is, the relaxation time of the dipole pair may be expressed as

$$\tau_B = \tau_{0B} e^{\Delta_B/T}, \quad (2)$$

with $\omega\tau_B \approx 1$ at the peak in $\delta\epsilon''$. The "barrier height" for the reorientation process is Δ_B in units of kelvin. Values of Δ , the prefactor τ_0 , and the temperature T_p at which the peak occurs are listed in Table I for peaks A , B , and C .

We attempt to model the frequency and temperature dependence of the features in ϵ' and in ϵ'' through the dispersion relation¹⁹

$$\epsilon' = \epsilon'_m + \sum_i \frac{a_i}{T} (1 + \omega^2\tau_i^2)^{-1} + \frac{b}{T}, \quad (3)$$

and

$$\epsilon'' = \sum_i \frac{a_i}{T} (\omega\tau_i)(1 + \omega^2\tau_i^2)^{-1}, \quad (4)$$

obtained from ϵ' by the Kramers-Kronig relation. The constants a_i are proportional to the concentrations of particular pairs of configurations. The subscripts i identify the subset of OH^- pairs responsible for peak $i = A, B$, or C . The term b/T of Eq. (3) is used somewhat arbitrarily to represent all "free" dipoles essentially not interacting with a neighboring OH^- ion in the temperature range of interest. The temperature dependencies of ϵ' and ϵ''

are contained both in the T^{-1} factors and in the temperature dependence of τ , Eq. (2).

Using Eq. (4), $\delta\epsilon'' = (a_B/T)(\omega\tau_B)(1 + \omega^2\tau_B^2)^{-1}$ has been calculated for peak B of the 1500 ppm sample. The results of this computation are compared with the measured data in Fig. 6. The only adjustable parameter in Fig. 6 is the constant a_B . The fit to the data is sufficiently good that we do not use alternative schemes employing additional adjustable parameters.²⁰ The fit for peak A of Fig. 2 is similar to that of peak B ; the fit for peak C is not as satisfactory and will be discussed later in this paper. The constants a_i and Δ_i for peaks A , B , and C of the 1500 ppm sample are listed in Table I. These same constants, a_i and Δ_i , can be used in Eq. (3) to compute ϵ' . The results of the computation agree satisfactorily with the data (such as the insert in Fig. 1), though, as explained previously, the A , B , and C features in ϵ' are less well resolved than in ϵ'' . The fact that the dispersion relations of Eqs. (3) and (4) agree with the data implies that dipole pairs do not interact with other dipole pairs. In view of the small concentration of dipole pairs, this is not a surprising result.

To determine the influence of strain and dislocations on ϵ' and ϵ'' , a crystal was intentionally deformed uniaxially by 4%. The peaks seen in Fig. 2 and labeled A , B , and C did not shift in temperature, but did decrease in magnitude by a factor of ≈ 2 when plotted versus T_{max} on a curve such as Fig. 4. Thus the introduction of dislocations removes a portion of the OH^- pairs from participation in the relaxation phenomena responsible for the peaks in ϵ'' . A 9-h anneal in argon of an undeformed crystal at a temperature of 1010 K, which is

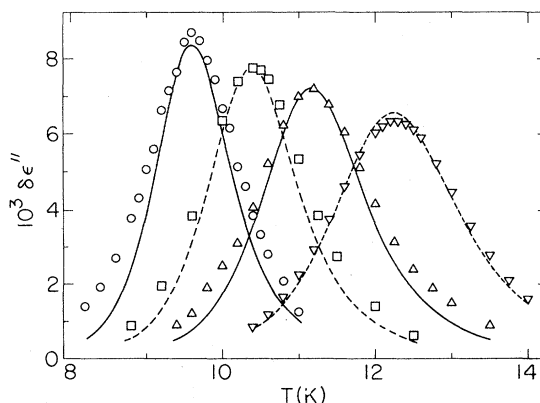


FIG. 6. Comparison between $\delta\epsilon''$ calculated from Eq. (4) and the measured values for the 1500-ppm sample of KCl:OH . \circ , \square , Δ , and ∇ were measured at frequencies of 200, 10^3 , 4×10^3 , and 2×10^4 Hz, respectively.

TABLE I. Parameters of the peaks *A*, *B*, and *C* found in Fig. 2 for a 1500 (at.) ppm sample of KCl:OH. For the frequency-dependent parameters T_p and $\delta\epsilon''$, a frequency of 4×10^3 Hz was used. The constant b is 12.4 K for this sample.

Peak	T_p (K)	τ_0 (sec)	Experimental				Theoretical			f
			Δ (K)	$\delta\epsilon''$	a (K)	a/b	c_i/c	(pair)		
<i>A</i>	66	2.0×10^{-14}	1400	8×10^{-3}	1.07	8.6×10^{-2}	0.6×10^{-2}	(<i>d</i> /2, <i>d</i> /2, 0)	8	
<i>B</i>	11.2	4.4×10^{-13}	205	7.2×10^{-3}	0.16	1.3×10^{-2}	0.6×10^{-2}	(<i>d</i> , <i>d</i> , 0)	8	
<i>C</i>	3.9	3.6×10^{-11}	54	4.1×10^{-2}	0.31	2.5×10^{-2}	2.4×10^{-2}	(<i>d</i> /2, <i>d</i> , 3 <i>d</i> /2)	32	
								1.8×10^{-2}	(<i>d</i> /2, <i>d</i> /2, <i>d</i>)	24
								0.6×10^{-2}	(3 <i>d</i> /2, 3 <i>d</i> /2, 0)	8
								0.6×10^{-2}	(<i>d</i> , <i>d</i> , <i>d</i>)	8

close to the melting temperature of 1050 K, did not alter significantly the low-temperature dielectric behavior.

Substitution of OD^- for OH^- did not alter the observed behavior of KCl near the peaks *A*, *B*, and *C*. This indicates that quantum-mechanical tunneling need not be considered explicitly in a description of the pair reorientation process.

Summarizing, the series of peaks seen in Fig. 2 is caused by dipole pairs which reorient in the applied electric field by thermal activation, and which obey the dispersion relations of Eqs. (3) and (4). To proceed further we need a model of the dipole pair. The model discussed below is speculative, but does produce a dielectric response which is in qualitative and nearly quantitative agreement with the experimental results.

The OH^- ion is known to enter substitutionally²¹ for the Cl^- ion in KCl for concentrations less than ≈ 5000 ppm. Such a defect experiences a crystal field having potential minima in the six [100] directions.²² The OH^- can tunnel between these minima, hence the sixfold degeneracy of the ground state is lifted. The existence of these tunneling states is consistent with results obtained from paraelectric resonance,²³ thermal conductivity,²⁴ and specific-heat^{5,25,26} measurements. The tunneling states themselves are not important in the present context. What is important is that the dipoles in KCl orient along [100] directions in the presence of small electric or stress fields, and can tunnel very rapidly through the intermediate barriers by 90° steps.²⁷ This explains the paraelectric behavior of the noninteracting dipoles in KCl at temperatures above ≈ 5 K.

Both electric and stress fields arise from the presence of an OH^- impurity, and hence there will be interactions between neighboring pairs of OH^- ions.

The resulting energy levels of an interacting pair of OH^- ions having an interdipolar axis of [110] are shown in Fig. 7 using the notation and computed energies given in Ref. 28. This notation is shown pictorially in Fig. 8. We will identify a particular configuration of dipoles by giving the position of one relative to the other. Thus the nearest-neighbor pair having an interdipole axis of [110] will be designated (*d*/2, *d*/2, 0) where *d* is the Cl^- - Cl^- separation along [100] in KCl.

It may be seen from Fig. 8 that the ground state $|3a\rangle$ of a (*d*/2, *d*/2, 0) pair has a net dipole moment of $\approx p$ along [100], the same moment as a single, OH^- ion in KCl. Furthermore, at least two discrete 90° jumps are required, one for each dipole, for the dipole pair to reorient into a second $|3a\rangle$ ground state with the dipole moment aligned in the

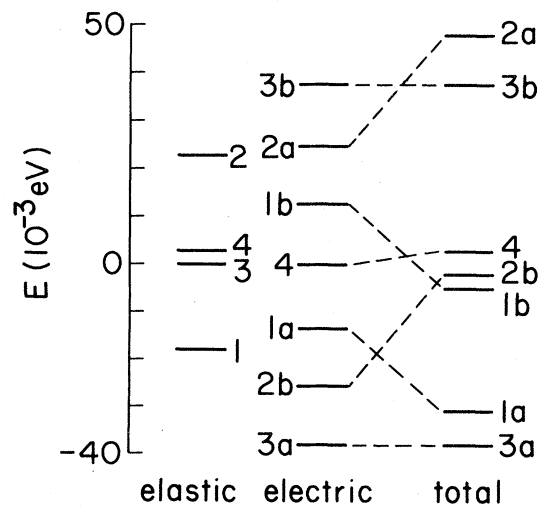


FIG. 7. Splitting of the energy levels of the nearest-neighbor OH^- - OH^- pair in KCl caused by elastic and electric interactions (Ref. 28).

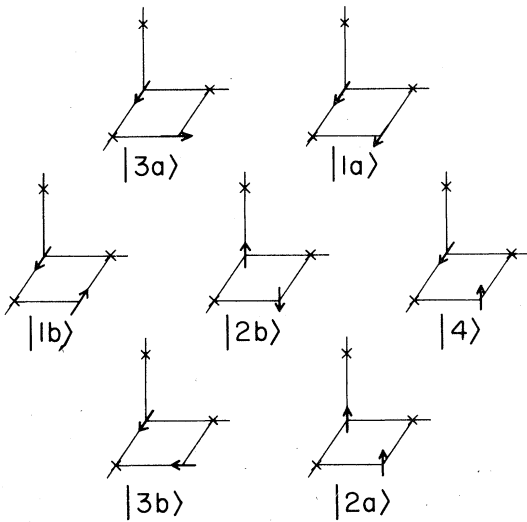


FIG. 8. Orientations of the two electric dipole moments for the nearest-neighbor OH⁻-OH⁻ pair in KCl. The notation is the same as that used in Fig. 7. Keeping one ion at the origin, there exist 11 other nearest-neighbor positions for the second ion. Each would have the same set of dipolar orientations shown here.

opposite direction. This reorientation process is shown in Fig. 9. There are other possible intermediate states, but those shown require the *least* energy. The reorientation is shown on an energy diagram in Fig. 10. Note that the intermediate state for the pair is $|1b\rangle$, not the lowest excited state $|1a\rangle$ of Fig. 7.

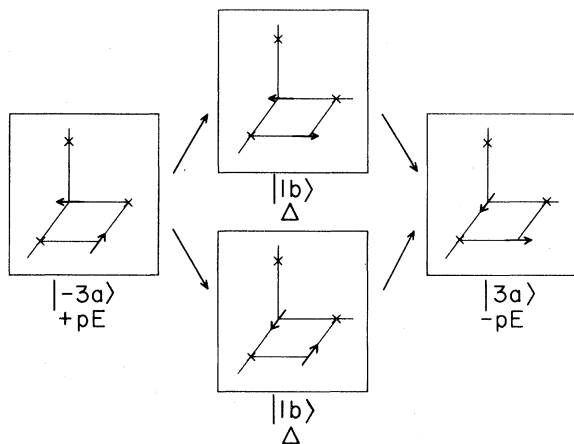


FIG. 9. Assuming an applied electric field directed to the right, this shows the process whereby a dipole pair reorients, via one of two degenerate intermediate states $|1b\rangle$, so that its electric dipole moment may be directed to the right. This process is shown on an energy-level diagram in Fig. 10.

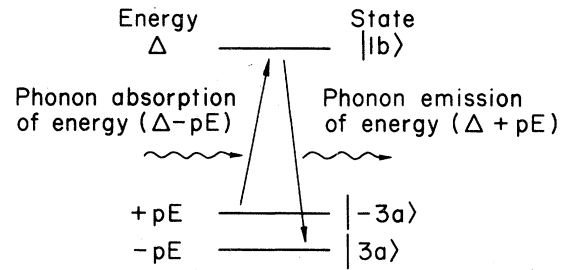


FIG. 10. The reorientation process of Fig. 9 is represented here on an energy-level diagram. The degenerate ground states $|3a\rangle$ have been slightly split by $2pE$, where p is the net electric dipole moment of the pair and E is the magnitude of the applied electric field.

Not all dipole pairs can reorient via a two-step process. For example, the ground state of the next-nearest-neighbor pair $(d,0,0)$ having an interdipolar axis of $[100]$ has both dipoles aligned in the same direction. This configuration requires four steps to reorient from one ground state to another in which the net dipole moment is reversed in direction. Such a high-order process is less probable. We therefore expect to detect only dipole pairs which reorient by two 90° steps.

The two-step relaxation process of Fig. 10, which involves a real intermediate state, has been considered theoretically.²⁹ It can occur by the absorption of a phonon having energy $\Delta - pE$ and the emission of a phonon having energy $\Delta + pE$. For $T < \Delta$ the relaxation time for this process is

$$\tau = B \Delta^{-3} e^{\Delta/T}, \tag{5}$$

where B is a constant. Comparison with Eq. (2) gives $\tau_0 = B \Delta^{-3}$. The empirical values of τ_0 and Δ have been listed in Table I. A plot of τ_0 versus Δ is shown in Fig. 11. The line is drawn with a slope of

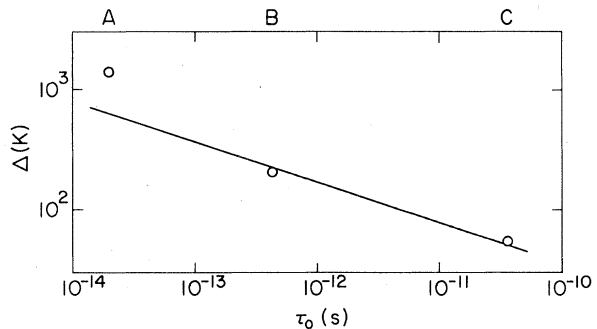


FIG. 11. Activation energy Δ versus prefactor τ_0 for peaks A, B, and C found in Fig. 2. The solid line shows the relationship between τ_0 and Δ expected from Eq. (5).

–3, and it may be seen that Eq. (5) gives a reasonable explanation for the factor of ≈ 2000 range in the prefactor τ_0 of Eq. (2). It would be awkward to explain this range of values for very similar defects in terms of an “attempt” frequency as is often done for other relaxation mechanisms. It will be noted in Fig. 11 that the datum for peak *A* lies above the line. This is to be expected since Eq. (5) is valid only for $\Delta < \Theta_D$, where Θ_D is the Debye temperature of ≈ 240 K for KCl.³⁰ When $\Delta > \Theta_D$ as for peak *A*, the temperature dependence of τ becomes less rapid.³¹ Thus $\tau_{0,A}$ should indeed fall above the line on Fig. 11.

Based on the foregoing discussion, we will assume that the peaks in Fig. 2 are caused by the two-step reorientation of dipole pairs, and will proceed next to inquire whether the number and magnitude of observed peaks is reasonable within this assumption.

For the nearest-neighbor ($d/2, d/2, 0$) pair, the energy Δ has been calculated in Ref. 28 and is shown in Fig. 7 as the difference between the $|3a\rangle$ and $|1b\rangle$ levels. The calculation gives $\Delta \approx 400$ K, and the values for pairs having OH^- ions of greater separation would be smaller. Yet the measured value for peak *A* is 1400 K. We will comment later on this difference in energies.

Since the computation presented in Ref. 28 does not provide numerical results consistent with the present data, we will compute *approximate* energy levels using three simplifying assumptions. First, it is assumed that the electric dipole-dipole interaction dominates over the elastic interaction and so the elastic contribution will be ignored. This avoids a significant complexity in the computation.³² Second, we assume that the electric interaction scales as r^{-3} and that the energy of interaction is given by³³

$$U = \frac{1}{4\pi\epsilon_0\epsilon'_m} \left[\frac{\vec{p}_1 \cdot \vec{p}_2}{r^3} - 3 \frac{\vec{p}_1 \cdot \vec{r} \vec{p}_2 \cdot \vec{r}}{r^5} \right], \quad (6)$$

where ϵ_0 is the free-space value of ϵ' and r is the separation between the two OH^- ions of the pair. Third, it is assumed that peak *A* is caused by the ($d/2, d/2, 0$) pair, and the product p^2/ϵ'_m in Eq. (6) is adjusted to give a $|3a\rangle$ to $|1b\rangle$ energy separation close to the measured Δ of Table I. With these assumptions the Δ listed in Table II have been obtained from Eq. (6). Using these values of Δ and Eq. (5), the temperatures T_p at which peaks should occur have been calculated and are included in Table II. Certain pairs, such as ($d, 0, 0$), are not listed in this table since they do not reorient by processes involving only two 90° steps.

From Table II it will be observed that discrete peaks in ϵ'' might be expected at temperatures near 61 and 10 K, while possibly four peaks fall near 4 K. These are close to the temperatures observed experimentally and listed in Table I. At greater physical separation of the OH^- ions ($n \geq 3$ in Table II) the peaks in ϵ'' become close together and cannot be resolved. They coalesce into peak *N* of Fig. 2. For reference purposes, note that a concentration of 1000 ppm corresponds to an average OH^- separation of $n \approx 10$ in Table II. At separations even somewhat less than $n \approx 10$, the pair interaction would cease to dominate and the influence of electric (and elastic) fields from other OH^- ions would have to be included. A mean-random-field approximation⁴ has attempted to do this.

The peak labeled *C* in Fig. 2 is replotted in Fig. 12 with the background subtracted. The data have been fitted to Eq. (4) as shown by the lines, the parameters Δ and τ_0 are listed in Table I. The peaks measured experimentally are much broader

TABLE II. Estimates of activation energy Δ computed assuming electric dipole-dipole interactions, and the corresponding temperature T at which a peak appears in ϵ'' as computed from Eq. (5) using $B = 4.74 \times 10^{-6}$ sec K^3 and a frequency of 4×10^3 Hz. Units are K. Since $1470 \text{ K} > \Theta_D$, Eq. (5) should not be used for that activation energy. The constant B has the same value for KCl:OD as for KCl:OH.

pair <i>n</i>	$\frac{1}{2}d(n, n, 0)$		$\frac{1}{2}d(n, n, 2n)$		$\frac{1}{2}d(2n, 2n, 2n)$		$\frac{1}{2}d(n, 2n, 3n)$	
	Δ	T_p	Δ	T_p	Δ	T_p	Δ	T_p
1	1470	(61)	71	4.8	50	3.6	46	3.4
2	184	10	8.9	1.0	6.3	0.8	5.7	0.8
3	55	3.9	2.3	0.5	1.9	0.5	1.7	0.5
4	23	2.0						
5	12	1.3						
6	6.8	0.9						
7	4.3	0.7						

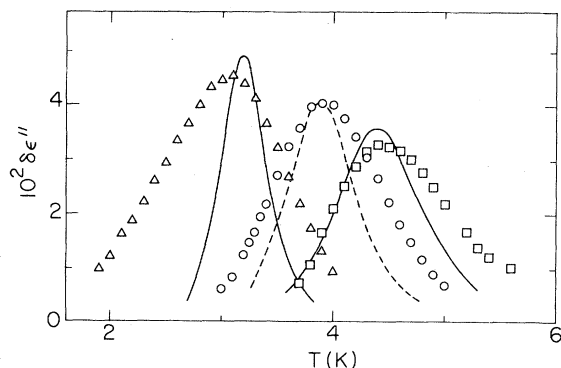


FIG. 12. Comparison between $\delta\epsilon''$ of peak C, calculated from Eq. (4), and the measured values for the 1500-ppm sample of KCl:OH. Δ , \circ , and \square were measured at frequencies of 200, 4×10^3 , and 2×10^4 Hz, respectively. The computation assumed a single relaxation mechanism, whereas Table II suggests three or four mechanisms. The presence of more than one relaxation mechanism could account for the widths of the peaks.

than the calculated peaks. This may be caused by the presence of two or more peaks near the same temperature as suggested in the last columns of Table I. But it must also be recognized that it is more difficult to estimate the background contribution under peak C, and hence subtraction of the background may widen (or narrow) the peak in $\delta\epsilon''$.

We should also be able to estimate the magnitude of $\delta\epsilon''$, that is, the constants a_i of Table I. In making this calculation, we assume initially that all Cl^- sites are equally probable for the substitution of an OH^- impurity. Not all ground-state configurations of pairs produce a net dipole moment in the direction of the applied field. For example, in Fig. 8 the ground state $|3a\rangle$ does not have a net dipole moment in the vertical direction. The number of sites which contribute to the dielectric response in a given direction are listed as \mathcal{N} in Table I. The concentration c_i of dipole pairs which contribute to ϵ'' is thus $c_i = c^2 \mathcal{N} / 2$, where again c is the concentration of OH^- ions. The calculated ratios of $c_i/c = c \mathcal{N} / 2$ are listed in Table I where they may be compared with the same ratio measured experimentally, namely a_i/b .

The computed ratio c_i/c for peak B is in reasonable agreement with the ratio a/b for that peak. For peak C, the ratio $a/b = 2.6 \times 10^{-2}$, whereas the ratio c_i/c might range from 2.4×10^{-2} to 5.4×10^{-2} depending on how precisely the four possible peaks listed in Table I fall near the same temperature. We note that the value of a/b for

peak A is a factor of 6.6 larger than for peak B, while the computed values of c_i/c suggest the ratio should be unity. This means that the $(d/2, d/2, 0)$ sites may have a higher probability of occupation than we have assumed. Part of the difference could occur during crystallization, since the $(d/2, d/2, 0)$ nearest-neighbor pair has an attractive interaction much larger than for other pairs. Taking this energy to be of order $\Delta_A \approx 1400$ K, the Boltzmann factor is $\approx e^{1400/1050} \approx 4$, where 1050 K is the melting (growth) temperature of KCl. Thus the population of $(d/2, d/2, 0)$ sites should be a factor of ≈ 4 larger than if calculated under the assumption that all Cl^- sites are equally probable for occupation by OH^- ions.

We have found that our model has provided a reasonable, nearly quantitative explanation for the series of peaks occurring in Fig. 2. All quantities are in agreement with previous data if available. For example, b of Eq. (1) may be written as

$$b = np^2/3\epsilon_0 k, \quad (7)$$

where n is the density of OH^- ions and k is the Boltzmann constant. Using our data we obtain $p = 4.1 \pm 0.3$ D ($1.38 \pm 0.1 \times 10^{-29}$ C m), which is close to that quoted in the literature.^{5,22} This value is, however, smaller by $\approx 35\%$ than the value of p obtained from Eq. (6) using $\epsilon'_m = 4.5$ and adjusting p^2/ϵ'_m so as to obtain the Δ values listed in Table II. It is not clear to us if the apparent enhancement of p^2/ϵ'_m by a factor of 2.4 deduced from the dipole-dipole interaction is consistent with local-field corrections³³ for substitutional impurities separated by a distance of $\approx d$, or if it reflects the complicated influence of elastic interactions between OH^- dipoles.³²

In completing this section, we wish to direct the readers attention to an analogous situation in systems of interacting magnetic dipoles. Crystalline $(\text{Eu}_x \text{Sr}_{1-x})\text{S}$ is a magnetic spin-glass for $x > 0.13$, the percolation threshold. Provided $x < 0.13$, a frequency- and concentration-dependent peak appears in the magnetic susceptibility. The peak obeys an Arrhenius law³⁴ as for KCl:OH. The authors account for this peak by assuming the freezing of nearest-neighbor magnetic dipole pairs.

SUMMARY

The reorientation of a pair of neighboring OH^- ions in KCl occurs via a thermally activated process. For certain pairs this appears to be a two-

phonon process, with each ion of the pair making one 90° step. A simple computation assuming an electric dipole-dipole interaction within the pair provides good agreement with the measured temperature, frequency, and concentration dependence, and apparently good agreement with the interion separation. The difficulty with this computation is the uncertain local-field correction for electric and elastic dipoles separated by a distance of order the lattice parameter. A subtle change in dielectric constant

associated with a low-temperature phase transition³⁵ has not been observed.

ACKNOWLEDGMENTS

The authors thank M. V. Klein and T. J. Rowland for providing some of the samples, and M. W. Klein, H. V. Beyeler, D. S. Matsumoto, and M. W. Grant for helpful conversations. This work was supported in part by the U. S. Department of Energy under Contract No. DE-AC02-76-ER01198.

- ¹V. Narayanamurti and R. O. Pohl, *Rev. Mod. Phys.* **42**, 201 (1972); F. Bridges, *Crit. Rev. Solid State Sci.* **5**, 1 (1975), and papers cited therein.
- ²Y. Farge and M. P. Fontana, *Electronic and Vibrational Properties of Point Defects in Crystalline Solids* (North-Holland, New York, 1979).
- ³F. Lüty, *J. Phys. (Paris)* **28**, C4-120 (1967), and papers cited therein.
- ⁴M. W. Klein, C. Held, and E. Zuroff, *Phys. Rev. B* **13**, 3576 (1976), and papers cited therein.
- ⁵A. T. Fiory, *Phys. Rev. B* **4**, 614 (1971).
- ⁶B. Fischer and M. W. Klein, *Phys. Rev. Lett.* **37**, 756 (1976).
- ⁷J. B. Hartman and T. F. McNelly, *Rev. Sci. Instrum.* **48**, 1072 (1977). We have not been successful in reproducing the feature observed in $d\epsilon'/dT$ near 0.7 K for KCl:OH.
- ⁸P. J. Anthony and D. S. Matsumoto (unpublished). The observation of a rounded, rather than a sharp, feature in ϵ' was attributed to a concentration gradient in the sample.
- ⁹Crystals were obtained from M. V. Klein and from the Crystal Growth Laboratory of the University of Utah.
- ¹⁰P. A. Anthony, Ph.D. thesis, University of Illinois, 1978 (unpublished).
- ¹¹R. J. Soulen, *J. Phys. (Paris)* **39**, C6-1166 (1978); J. F. Schooley, *ibid.* **39**, C6-1169 (1978).
- ¹²A. C. Anderson, R. E. Peterson, and J. E. Robichaux, *Rev. Sci. Instrum.* **41**, 528 (1970).
- ¹³Similar data are not available for KCl:OD. We did find T_{\max} of our 250- and 5000-ppm samples to be proportional to the estimate of concentration content provided by the crystal grower.
- ¹⁴W. Kanzig, H. R. Hart, and S. Roberts, *Phys. Rev. Lett.* **13**, 543 (1964).
- ¹⁵A. T. Fiory, *Rev. Sci. Instrum.* **42**, 930 (1971).
- ¹⁶M. V. Klein, private communication.
- ¹⁷R. A. Brand, S. A. Letzring, H. S. Sack, and W. W. Webb, *Rev. Sci. Instrum.* **42**, 927 (1971), and references cited therein.
- ¹⁸P. A. Varotsos, *J. Phys. Lett. (Paris)* **39**, L79 (1978).
- ¹⁹W. Kauzmann, *Rev. Mod. Phys.* **14**, 12 (1942), and papers cited therein.
- ²⁰A. K. Jonscher, *J. Phys. D* **13**, L89 (1980), and papers cited therein.
- ²¹H. Paus and F. Lüty, *Phys. Status Solidi* **12**, 341 (1965).
- ²²U. Kuhn and F. Lüty, *Solid State Commun.* **2**, 281 (1964).
- ²³W. E. Bron and R. W. Dreyfus, *Phys. Rev.* **163**, 304 (1967), and papers cited therein.
- ²⁴M. Locatelli, *Phys. Lett.* **61A**, 185 (1977), and papers cited therein.
- ²⁵I. W. Shepherd, *J. Phys. Chem. Solids* **28**, 2027 (1967).
- ²⁶P. P. Peressini, J. P. Harrison, and R. O. Pohl, *Phys. Rev.* **182**, 939 (1969).
- ²⁷F. Lüty, *J. Phys. (Paris)* **34**, C9-49 (1973).
- ²⁸R. T. Shuey and H. U. Beyeler, *Z. Angew. Math. Phys.* **19**, 278 (1968).
- ²⁹R. Orbach and H. Stapleton, in *Electron Paramagnetic Resonance*, edited by S. Geschwind (Plenum, New York, 1972), p. 121.
- ³⁰J. R. Hardy and A. M. Karo, *The Lattice Dynamics and Statics of Alkali Halide Crystals* (Plenum, New York, 1979).
- ³¹R. L. Marchand, *Phys. Rev. B* **9**, 4613 (1974).
- ³²B. G. Dick, *Bull. Am. Phys. Soc.* **26**, 268 (1981), and (unpublished).
- ³³G. D. Mahan, *Phys. Rev.* **153**, 983 (1967).
- ³⁴G. Eiselt, J. Kotzler, H. Maletta, D. Stauffer, and K. Binder, *Phys. Rev. B* **19**, 2664 (1979).
- ³⁵It should be noted that the behavior of ϵ calculated in Ref. 6 was for $\omega = 0$, whereas the present measurements used $\omega/2\pi \geq 10^2$ Hz.